

2006

Numerical Simulation and Experimental Comparison of Refrigeration and Air Conditioning Scroll Compressors. Application to Trans-Critical Carbon Dioxide Cycles

J. Rovira

Universitat Politecnica de Catalunya

Joaquim Rigola

Universitat Politecnica de Catalunya

Asseni Oliva

Universitat Politecnica de Catalunya

Carlos D. Perez-Segarra

Universitat Politecnica de Catalunya

Follow this and additional works at: <http://docs.lib.purdue.edu/icec>

Rovira, J.; Rigola, Joaquim; Oliva, Asseni; and Perez-Segarra, Carlos D., "Numerical Simulation and Experimental Comparison of Refrigeration and Air Conditioning Scroll Compressors. Application to Trans-Critical Carbon Dioxide Cycles" (2006). *International Compressor Engineering Conference*. Paper 1801.
<http://docs.lib.purdue.edu/icec/1801>

This document has been made available through Purdue e-Pubs, a service of the Purdue University Libraries. Please contact epubs@purdue.edu for additional information.

Complete proceedings may be acquired in print and on CD-ROM directly from the Ray W. Herrick Laboratories at <https://engineering.purdue.edu/Herrick/Events/orderlit.html>

Numerical Simulation and Experimental Comparison of Refrigeration and Air Conditioning Scroll Compressors. Application to Trans-critical Carbon Dioxide Cycles

J. ROVIRA, J. RIGOLA, A. OLIVA, C.D. PÉREZ-SEGARRA

Centre Tecnològic de Transferència de Calor (CTTC),
Universitat Politècnica de Catalunya (UPC)
ETSEIAT, C/Colon, 11, 08222, Terrassa, (Barcelona), Spain
Tel. +34-93-739.81.92; FAX: +34-93-739.89.20
e-mail: cttc@cttc.upc.edu; <http://www.cttc.upc.edu>

ABSTRACT

A numerical simulation model of scroll compressors has been developed to obtain temperature, pressure, and mass flow rate maps evolution, solving continuity, momentum and energy equations. Chamber volumes, areas and leakages calculus have been programmed following (Halm, 1997) formulation. Chen's (2004a)(2004b) thermal resistances have been introduced in the model for the whole compressor thermal treatment. Fluid properties are calculated from (REFPROP, 1998) database for each volume.

To validate the numerical model presented, several experimental results of (Halm, 1997) and (Park, 2002) have been compared, considering R22 as a working fluid. The general comparisons obtained have shown a reasonable good agreement.

A first illustrative CO₂ results are presented and compared against R22 standard compressor. The results show the possibilities of CO₂ for refrigeration and air conditioning applications. The influence of some aspects has also been studied.

1. INTRODUCTION

Some overall models are used in the technical literature, but no one focus on fluid thermal treatment including leakages. This new overall model is focused on thermal treatment of fluid temperature, during all compression process. Leakages have been also taken into account, due their effects in reducing volumetric efficiency, increasing power consumption, reducing mass flow rate and increasing discharge temperature. This effect is more important when carbon dioxide is used as fluid refrigerant.

In the numerical model presented, wall temperature of aluminum and steel scrolls is considered together with the block temperature, changing along the simulation execution like other compressor components. A thermal model for the whole compressor has been developed following (Halm, 1997), although using Chen's (2004a)(2004b) values for thermal resistances and incorporating the fluid properties evaluation from NIST (REFPROP, 1998) 6.01 database, with the possibility of simulating the compressor using all available fluid refrigerants.

2. MODEL DESCRIPTION

The program first calculates volumes and areas, with the formulation described below. Then, it solves every chamber at every crank angle degree to complete one turn. At each angle, all chambers are solved simultaneously, calculating leakages, densities, pressures and temperatures several times until angle convergence is reached. A comparison of temperature, pressure and density maps with the previous turn are carried out, to obtain a global convergence. Once the solution is completed, the program evaluates compression work and efficiency calculus to show both global and detailed final results obtained. Figure 1 shows the flow diagram of the numerical model.

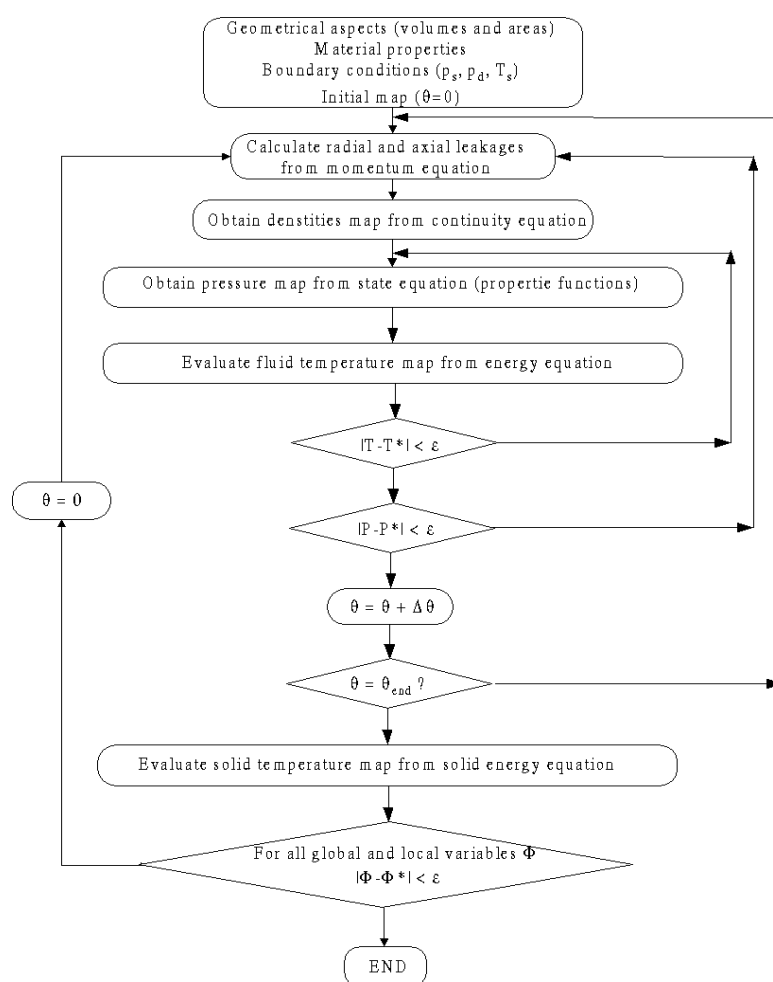


Figure 1: Program Flow Diagram

2.1 Fluid Thermal Model

Changes in fluid temperature are due to changes in suction, compression and discharge volumes (1)(2)(3), pressure, heat exchanged with walls and leakages. This last aspect is presented as a novelty in the present paper. All of them are correlated with each other. The program solves all chambers, at each crank angle degree, simultaneously, until convergence of leakages, densities, pressures and temperatures are reached. Fluid properties are considered as functions of pressures and temperatures. In order to reduce CPU time, properties are not obtained directly from REFPROP database, and are pre-calculated feeding a property matrix of 250x250 points. Then, a property value is obtained by interpolation of four adjacent points. The selected number of points assures accurate evaluation of the thermo-physical properties.

2.2 Geometrical aspects

The suction, compression and discharge chamber volumes are geometrically designed as follows:

$$V_s = \frac{1}{2} h r_b r_o \left((2\theta\varphi_e - \theta^2 - \frac{3}{2}\theta\pi) - 2(\varphi_e - \pi) \sin \theta - \frac{\pi}{4} \sin 2\theta + 2(1 - \cos \theta) \right) \quad (1)$$

$$V_c = \pi h r_b r_o \left(2\varphi_e - 2\theta - \frac{7}{2}\pi \right) \quad (2)$$

$$V_{d-dd} = h r_b r_o \left(5(\varphi_k^2 - \varphi_{is}^2) - \frac{11\pi}{2}(\varphi_{is} - \varphi_k) \right) + V_{cl} \quad (3)$$

where the clearance volume is evaluated as $V_{cl} = h r_c^2 \left(\pi - \sin^{-1} \frac{2r_b}{r_c} - \frac{2r_b}{r_c} \right)$

and the involute angle φ_k is evaluated as : $\varphi_k = \begin{cases} \varphi_e - 2\pi - \theta & \text{if } 0 \leq \theta \leq \theta_d \\ \varphi_e - \theta & \text{if } \theta_d \leq \theta \leq 2\pi \end{cases}$

2.3 Leakages

The two kind of leakages presented in scroll compressor have been considered. The flank, or tangential, leakage occurs between two scrolls in the contact point, where δ_f is the flank leakage gap ($\delta_f=10.0e-6m$); while the radial leakage occurs between the scroll and both top and bottom plates. These leakages have a gap named δ_r ($\delta_r=2.1e-6m$).

The inlet area A_{in} (the surface between plateau and scroll) and the outlet area A_{out} (the surface towards the external chamber) of the two radial leakages between the neighboring chambers are respectively:

$$A_{in} = \delta_r \int_{\varphi_k}^{\varphi_{k+1}} L_o d\varphi \quad (4)$$

Substituting L_o

$$A_{in} = \delta_r \int_{\varphi_k}^{\varphi_{k+1}} r_b (\varphi - \varphi_{o0}) d\varphi \quad (5)$$

Integrating (if $\varphi_{o0}=0$)

$$A_{in} = \delta_r r_b \frac{1}{2} (\varphi_{k+1}^2 - \varphi_k^2) \quad (6)$$

$$A_{out} = \delta_r \int_{\varphi_k}^{\varphi_{k+1}} L_i d\varphi \quad (7)$$

Substituting L_i

$$A_{out} = \delta_r \int_{\varphi_k}^{\varphi_{k+1}} r_b (\varphi - \varphi_{i0}) d\varphi \quad (8)$$

Integrating ($\varphi_{i0}=\text{constant}$)

$$A_{out} = \delta_r r_b \left\{ \frac{1}{2} [(\varphi_{k+1})^2 - (\varphi_k)^2] + [-\varphi_{i0}(\varphi_{k+1}) + \varphi_{i0}(\varphi_k)] \right\} \quad (9)$$

For flank leakage: $A_{in}=A_{out}=h\delta_f$ (10)

Once, we have calculate the area, the fluid flow can be known by,

$$\dot{m} = \psi A_s \sqrt{2P_h \rho_h} \sqrt{\frac{\kappa}{\kappa+1} \left[\left(\frac{P_l}{P_h} \right)^{\frac{2}{\kappa}} - \left(\frac{P_l}{P_h} \right)^{\frac{\kappa+1}{\kappa}} \right]} \quad (11)$$

except for the critical pressure ratio:

$$\left(\frac{P_l}{P_h} \right) = \left(\frac{2}{\kappa+1} \right)^{\frac{\kappa}{\kappa-1}} \quad (12)$$

where P_l is the pressure in the low side, P_h is the pressure in the high side, A_s is the leakage area, ψ is a coefficient set at 0.08 by (Kim, 1998), and $\kappa=C_p/C_v$, evaluated using the fluid properties.

2.4 Compressor Solid Thermal Model

Following (Halm, 1997) and Chen's (2004a)(2004b) thermal resistance values, the model evaluating the different blocks of metal with heat exchange between oil, gas and metal objects is presented. The heat is generated in the motor and in the scrolls, and friction heat is also produced in scrolls and oil. The heat generated depends on the calculated compression work (W_{cp}) and the mechanical and electrical efficiencies evaluated from different available expressions of the literature.

2.5 Fusion of Discharge Chamber

Fusion of the "old" discharge chamber with the last two compression chambers, one of each scroll arm, occurs in every turn, creating the "new" discharge chamber, with the new volume equal at the volumes of three previous chambers, equaiotn (3), and the pressure and density calculated by averages pondered by mass.

2.6 Compression Work

Some authors like (Halm, 1997) uses a simple formula to calculate the compression work from the theoretical isentropic work. It is more real to evaluate directly the compression work from equation 13 if the numerical simulation model allows to know at each crank angle degree the pressure and volume evolution like the model here presented.

$$W_{cp} = \oint p dV \quad (13)$$

This evaluation is necessary for each chamber at each angle increment, as increment average of pressure multiplied by the volume increment. Adding all compression works for the whole turn it is possible to obtain the global compression work. In the numerical simulation model presented, small variations on compression work appear in the fusion chamber, due to not perfect matching of volume formulae and the difficulty in assign an average pressure for the fusion increment.

2.7 Efficiency

Defining the power consumption as compressor efficiencies multiplied by compression work, it can be established:

$$\dot{W}_E = \eta_m \eta_e \dot{W}_{cp} \quad (14)$$

Compression work absorbs the ancient isentropic work and adiabatic efficiency, because they are included in pressure and volume values calculus. Assigning motor electric efficiency as (Park, 2002) in equation (14) and a mechanical efficiency (Cho, 1996) ($\eta_m=92.3\%$), the program can guess the electric Power Consumption.

$$\eta_e = 0.6980 + 0.0013f + 4.1235 \cdot 10^{-5} f^2 - 4.8781 \cdot 10^{-7} f^3 + 1.4206 \cdot 10^{-9} f^4 \quad (15)$$

The power consumption is also used by the program in order to calculate the heat fluxes and temperatures until the global convergence program is reached.

2.8 Considerations and limitations of this model

Although the present numerical simulation model show some novelties in comparison with the other models here referenced, like the leakage consideration through all compression process and some improvements on equations used, there is some other aspects that limit the model and that must be taken into account: the present model is only valid for an entire number of scroll turns; the thermal effect of leakages to the entry channel have not been considered, the wall temperature is considered equal on both scroll solids, due to the temperature for all block is uniform. However, an important aspect like the fusion of the three central chambers is considered instantaneously at each crank angle degree.

3. MODEL VALIDATION

To validate the numerical model described, two different comparative have been carried out. The first one shows the nine experimental cases (Halm, 1997) considering different ranges of condensation and evaporation working condition. The second one shows five experimental cases (Park, 2002) with the same boundary conditions, only varying the mean real working frequency.

3.1 Comparative results at different working conditions

The nine experimental cases compared are evaluated under a frequency of 60Hz. The numerical results have been obtained considering the motor efficiency and electrical power, from the isentropic work (Halm, 1997). Table 1 shows the comparative numerical results obtained against the experimental data.

Table 1: Comparative numerical results vs. experimental data (Halm, 1997)

R22 T _{sh} = 10°C f = 60Hz T _{amb} = 25°C		T _c = 25C P _c = 1044KPa		T _c = 35C P _c = 1354KPa		T _c = 45C P _c = 1728KPa	
		<i>experimental</i>	<i>numerical</i>	<i>experimental</i>	<i>numerical</i>	<i>experimental</i>	<i>numerical</i>
T _e = -10.0C	\dot{m}	44kg/h	40.0kg/h	43kg/h	39.47kg/h	42kg/h	38.85kg/h
T _{in} = 0.0C	T _{dis}	80°C	75.9°C	92°C	87.88°C	105°C	98.76°C
P _e = 354KPa	\dot{W}_E	840W	857W	955W	1000W	1074W	1121W
	\dot{W}_{is} \dot{W}_{cp}	358W	404W	447W	508W	530W	620W
T _e = 0°C	\dot{m}	62kg/h	56.02kg/h	60kg/h	55.50kg/h	59kg/h	54.88kg/h
T _s = 10.0°C	T _{dis}	69°C	65.64°C	81°C	75.47°C	91°C	84.52°C
P _e = 497KPa	\dot{W}_E	817W	779W	936W	915W	1055W	1018W
	\dot{W}_{is} \dot{W}_{cp}	341W	400W	459W	514W	543W	642W
T _e = 10°C	\dot{m}	83kg/h	76.53kg/h	81kg/h	76.00kg/h	79kg/h	75.38kg/h
T _s = 20.0°C	T _{dis}	63°C	61.54°C	73°C	70.20°C	83°C	77.86°C
P _e = 680KPa	\dot{W}_E	804W	734W	923W	887W	1029W	981W
	\dot{W}_{is} \dot{W}_{cp}	258W	413W	417W	510W	569W	645W

The results of Table 1 show that differences on mass flow rate are lower than 10% in all studied cases, while the numerical model always under-predicts the experimental data. The discharge temperature is always numerically under-predicted with differences between 3 and 6%. Finally, the power consumption differs from an over-prediction of 8% to an under-prediction of 4%. Then, the result shows a reasonable good agreement with the maximum and minimum discrepancies at the condenser temperature of 25°C and 45°C, respectively.

3.2 Comparative results at different working frequencies

The five experimental cases compared have been evaluated under the ASHRAE-T boundary conditions changing the real mean working frequency. In these cases, the numerical simulation model has evaluated the mechanical efficiency proposed by (Cho, 1997) (92.3%) and the electrical efficiency of equation (12) (Park, 2002). Table 2 shows the scroll compressor geometry, while Table 3 shows the boundary conditions. Finally, Table 4 shows the comparative results of the five presented cases with a reasonable good agreement.

Table2: Scroll compressor dimensions.

Base circle radius	0.001703m
Thickness	0.00280m
Height	0.01852m
Displacement volume	11.49cm ³
Involute inner start angle	4.8857rad
Involute outer start angle	1.9024rad
Involute end angle	16.5000rad
Pitch	0.01070m
Orbiting radius	0.002550m

Table3: Boundary conditions.

Suction Pressure	625.95 kPa
Discharge Pressure	2145.99 kPa
Suction Temperature	35.0°C
Ambient Temperature	35.0°C

Table 4: Comparative numerical results vs. experimental data (Park, 2002)

	f=45		f=60		f=75		f=90		f=105	
	exp	num	exp	num	exp	num	exp	num	exp	num
\dot{W}_{cp}	459W		657W		888W		1163W		1495W	
η_{me}	72.96%		76.73%		80.01%		82.21%		83.01%	
\dot{W}_E	750W	629W	900W	856W	1200W	1109W	1500W	1414W	1800W	1801W
T_{dis}	124°C	119°C	118°C	121°C	121°C	123°C	126°C	126°C	132°C	130°C
\dot{m}	36 kg/h	37.83	51 kg/h	53.45	63 kg/h	70.44	69 kg/h	88.77	75kg/h	109.33

The results of Table 4 shows a quite good agreement on power consumption and discharge compressor temperature lower than 10% in all cases, although with significant differences on mass flow rate, specially at high frequencies of 90 or 105Hz. The minimum discrepancies of discharge temperature, power consumption and mass flow rate take place at the frequency of 60Hz.

4. CO₂ NUMERICAL RESULTS

4.1 Carbon dioxide scroll compressor numerical prototype

In order to show the possibilities of carbon dioxide as fluid refrigerant substitute, the same compressor of Table 2 has been considered only reducing the scroll height from 0.01852m to 0.00600m and the corresponding suction volume at 3.75cm³, to have a numerical model with a similar capacity or equivalent mass flow rate. Table 5 shows the nine cases simulated, which have been selected with the boundary conditions of Table 1 modifying the discharge pressure ranging between 8 and 10 MPa and using CO₂ as the working fluid refrigerant, following (Ishii, 2002) example. Suction pressures correspond to equilibrium liquid-vapor at the chosen evaporation temperatures.

Table 5: Carbon dioxide scroll compressor numerical results.

CO ₂ T _{sh} = 10°C f = 60Hz T _{amb} = 25°C		P _{dis} = 8.0MPa	P _{dis} = 9.0MPa	P _{dis} = 10.0MPa
T _{ev} = -10C T _s = 0.0C P _{ev} = 2.6487MPa	\dot{m} T_{dis} \dot{W}_{cp} η_{me} \dot{W}_E	48.26 kg/h 84.90C 825W 76.80% 1074W	47.94 kg/h 95.52°C 940W 76.74% 1225W	47.63 kg/h 105.53°C 1050W 76.67% 1370W
T _{ev} = 0C T _s = +10.0C P _{ev} = 3.4851MPa	\dot{m} T_{dis} \dot{W}_{cp} η_{me} \dot{W}_E	65.71 kg/h 74.74°C 779W 76.93% 1013W	65.34 kg/h 84.70°C 907W 76.88% 1180W	65.00 kg/h 94.21°C 1031W 76.83% 1353W
T _{ev} = +10C T _s = +20.0C P _{ev} = 4.5022MPa	\dot{m} T_{dis} \dot{W}_{cp} η_{me} \dot{W}_E	88.70 kg/h 66.68°C 712W 77.02% 924W	88.29 kg/h 75.42°C 845W 76.98% 1097W	87.89 kg/h 83.89°C 976W 76.94% 1268W

The results of Table 5 in comparison with the numerical and experimental data of Table 1 show that in all cases the mass flow rate increases between 6 and 8% when carbon dioxide compressor is considered, although power consumption increases around 10% with a maximum of 20%. Despite the results of the power consumption the possibilities to improve motor efficiency and reduce mechanical losses and fluid flow leakages can increase mass flow rate and reduce power consumption in order to obtain a CO₂ scroll compressor with comparable COP.

5. CONCLUSIONS

A numerical simulation of the thermal and fluid dynamic behavior of scroll compressors is presented. The model has been validated against different experimental data by (Halm, 1997) and (Park, 2002), showing the good predictions of the numerical results. Although the numerical results presented have used R22 and CO₂ as fluid refrigerant, the model allows working with any of the different available fluid refrigerants of the properties program table. A set of results with carbon dioxide has also been obtained with the aim to be compared against conventional scroll compressors. The results show the differences between both compressors and the necessity to improve the CO₂ compressors to obtain equal efficiencies.

NOMENCLATURE

f	Frequency (Hz)	V_c	Compression chamb. volume (m ³)
h	Height of scroll vanes (m)	V_{cl}	Clearance volume (m ³)
k	Isentropic coefficient (-)	V_{d-dd}	Volume of entire discharge region
\dot{m}	Refrigerant mass flow rate (kg/h)	V_s	Suction volume (m ³)
p	Pressure (MPa)	Greek symbols	
r_b	Involute basic circle radius (m)	φ_e	Involute ending angle
r_c	Radius of circular arc inner dis. ch.	φ_{is}	Inner involute starting angle
r_o	Radius of circular arc outer dis. ch.	φ_k	Involute angle at k point
T	Temperature (C)	η_e	electrical efficiency (%)
\dot{W}_{cp}	Compression Work (W)	η_m	mechanical efficiency (%)
\dot{W}_E	Electrical Power (W)	θ	Scroll orbiting angle

REFERENCES

- Chen. Y., Groll E.A., Braun J.E., 2004a, Modeling of Hermetic Scroll Compressors: Model Development, HVAC&R Research, Vol. 10, Num. 2, April, 2004.
- Chen. Y., Groll E.A., Braun J.E., 2004b, Modeling of Hermetic Scroll Compressors: Model Validation and Application, HVAC&R Research, Vol. 10, Num. 3, July, 2004.
- Halm, N.P., 1997, Mathematical Model of Scroll Compressor, Master Thesis, Herrick Laboratories, Purdue University.
- Ishii, Noriaki, et alli, 2002, Efficiency Simulations of a Compact CO₂ Scroll Compressor and its Comparison with same Cooling Capacity R410A Scroll Compressor, International Compressor Engineering Conference at Purdue, West Lafayette, Indiana, USA.
- Kim, Yongchan, Seo Kook-Jeong, Park Hong-Hee, 1998, Modeling on the Performance of an Inverter Driven Scroll Compressor, International Compressor Engineering Conference at Purdue, West Lafayette, Indiana, USA.
- Park Y. C., Kim Y. C., Cho H. H., 2002, Thermodynamics on the Performance of a Variable Speed Scroll Compressor with Refrigerant Injection. *Int. J. Refrigeration* 25, p. 1072-1082.
- REFPROP V6.01, NIST, Thermodynamic Properties of Refrigerants and Refrigerant Mixtures Database, National Institute of Standards and Technology, Standard Reference Program, Gaithersburg, MD, USA, July, 1998.
- Wang. B., 2005, A General Geometrical Model of Scroll Compressors Based on Discretional Initial Angles of Involute, *Int. J. Refrigeration* 28, p. 958-966.
- Winandy E., Saavedra O.C., Lebrun J., 2002, Experimental Analysis and Simplified Modeling of a Hermetic Scroll Refrigeration Compressor, *Appl. Therm.* 22, p.107-120.
- Yang-Hee Cho, Bye-Chul Lee, Jin-Kab Lee, 1996, Development of High Efficiency Scroll Compressor for Package Air Conditioners, International Compressor Engineering Conference at Purdue, West Lafayette, Indiana, USA.